Journal of Visual Communication and Image Representation **11**, 360–373 (2000)
doi:10.1006/jvci.1999.0451, available online at http://www.idealibrary.com on IDEAL®

Interresolution Look-up Table for Improved Spatial Magnification of Image

Guoping Qiu

School of Computer Studies, University of Leeds, Leeds LS2 9JT, United Kingdom
E-mail: qiu@scs.leeds.ac.uk

Received January 27, 1997; accepted September 8, 1999

The most commonly used image magnification techniques are interpolation based: nearest neighbor, bilinear, and bicubic. The drawbacks of these traditional methods are that images magnified by the simple nearest neighbor method often appear "blocky," while images magnified by linear and cubic interpolations usually appear "blurry." In this work, a new technique, which improves the performance of the traditional image magnification methods, is presented. We show how a differential image pyramid is first constructed using traditional interpolation methods, then how a vector quantizer is designed using the pyramidal data. The vector quantizer is a look-up table, termed the interresolution look-up table (IRLUT), which uses the lower resolution image vector as input to find as its output the corresponding higher resolution image vector. The improved image is produced by using the IRLUT's outputs to compensate for the image magnified by the traditional methods. Experimental results which show that images generated by the current method have sharper edges as well as lower reconstruction mean-square errors than those produced by traditional methods are presented.

1. INTRODUCTION

Image magnification is widely used in many aspects of image processing; examples include pyramid coding [1], computer graphics [2], shape restoration [3], and video processing [4]. The most commonly used techniques for image magnification are interpolation based. The simplest technique is the nearest neighbor (zero order) interpolation [5]. However, the magnified images produced by this technique often appear "blocky"; i.e., the pixels are visible as large blocks. This undesired effect is more striking when the zooming factor is high. Smooth images can be generated by using higher order interpolations. A commonly used approach is the bilinear interpolation [5, 6], which linearly interpolates along each row of the image, and then linearly interpolates the result along the column direction. Even smoother images can be produced by using cubic spline interpolation [6–8]. However, these methods smooth flat as well as edge areas; important visual features such as sharp edges

1047-3203/00 $35.00

and thin lines are smoothed over by the interpolations and the magnified images appear "blurry." Therefore, the results of these methods are often unsatisfactory.

Recently, researchers have proposed various improved algorithms for image magnification. For example, Huang and Chen [2] proposed a hybrid interpolation filtering method, Unser *et al.* [8] developed more accurate spline interpolation algorithms, Schultz and Stevenson developed a Bayesian approach to image enlargement [9], and Jensen and Anastassiou [10] used an edge fitting model to enlarge images. The main goal of these methods is to preserve the visual integrity in detailed areas of the magnified image, because interpolations blur the magnified image. To various extents, better results were reported by these authors.

This paper proposes a new method to improve the performance of traditional interpolation-based image magnification methods. Starting from a pyramidal model for multiresolution representation of an image, we observe the relationship of images at different resolutions. From this model, a new technique for image magnification is proposed. The new method introduces the concept of a compensation image, which is used to compensate the components of the magnified image that are lost during the interpolation process. The original contributions of this work also include the use of vector quantization to generate the compensation image. We will provide experimental results to demonstrate the improvements achieved by the proposed technique.

The rest of the paper is organized as follows. Section 2 will describe a pyramid model for the multiresolution representation of images. The new technique for image magnification based on the multiresolution image representation model is described in Section 3. The use of vector quantization for the implementation of the new image magnification technique is described in Section 4. Section 5 provides experimental results to demonstrate the effectiveness of the new technique. Finally, some conclusions of the work are presented in Section 6.

2. MULTIRESOLUTION REPRESENTATION OF IMAGE

Multiresolution representation of an image is widely used in image processing and computer vision. Amongst various schemes, pyramid structure is a popular form of multiresolution representation. To form a pyramid, an image is successively reduced in size through downsampling. Depending on the application, the downsampling process usually involves some form of filtering before subsampling the image. Figure 1 shows a three-level pyramid,

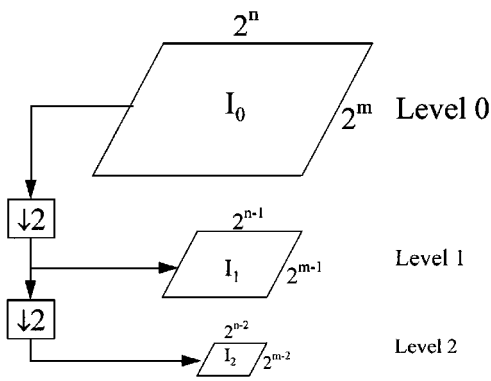

FIG. 1. A three-layer image pyramid; the higher level image is generated by downsampling the lower level image by a factor of 2 in both dimensions.

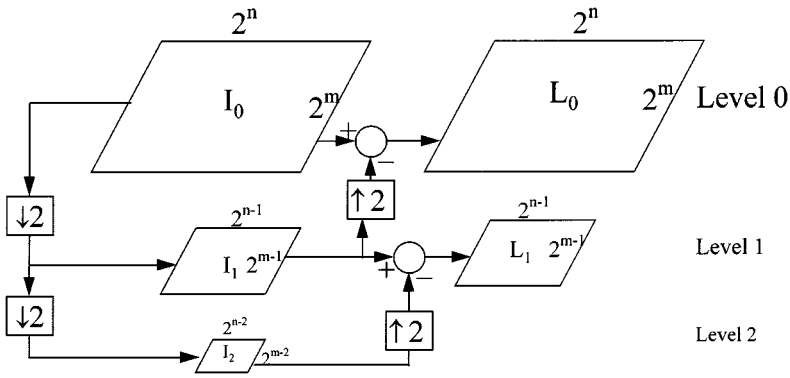

FIG. 2. A three-layer pyramid with difference images.

where the image is successively reduced in size by a factor of 2 in both dimensions. For convenience, we will only consider the case of magnification by a zooming factor of 2^k, where k is an integer.[1]

The downsampling (image reduction) process can also be implemented by interpolation [11, 12]. The principle of image reduction and magnification has been discussed in many textbooks; for example, readers can refer to the excellent books by Gonzalez and Woods [11, Section 5.9] and Pratt [12, Chapter 14]. To keep the writing concise, we shall omit the description of interpolation techniques for image reduction and enlargement.

The magnification process is the reverse operation of Fig. 1. For example, by magnifying level 1 image I_1 by a factor of 2 in both dimensions, the magnified image $\tilde{I}_0$ will be the same size as level 0 image I_0. However, due to the loss of information during the downsizing process, the magnified image $\tilde{I}_0$ will not be identical to the original image I_0. To completely represent I_0, we can use I_1 and a difference image between I_0 and $\tilde{I}_0$; the difference image is calculated as $L_0 = I_0 - \tilde{I}_0$. Figure 2 shows how the difference images at different levels are created.

An important observation of Fig. 2, which also motivates the development of the new method, is as follows. For an image of some given resolution which is to be magnified, it can always be assumed that the given image is obtained from an image of higher resolution by some downsizing methods. In this work, it is assumed that the downsizing is implemented using some form of interpolation.[2] With reference to Fig. 2, assume the given image is I_1, which is to be magnified by a factor of 2 in both dimensions. Ideally, the magnified image $\tilde{I}_0$ should be identical to I_0, from which I_1 is generated. However, from the discussions above, it is known that due to the lost of information in the process, there will be differences between $\tilde{I}_0$ and I_0. This difference provides a measure of how well a particular magnification method performs: the larger the difference, the poorer the performance of the technique. Conversely, the smaller the difference, the more accurate the magnification method. Therefore, in order to magnify an image, the goal we should aim at is to reduce the difference between $\tilde{I}_0$ and I_0.

From Figure 2, I_0 can be exactly represented by $\tilde{I}_0$ and L_0; i.e.,

$$I_0 = \tilde{I}_0 + L_0. \tag{1}$$

[1] It should be noted that although we study zooming factors of 2^k in this paper, the technique developed here could also be applied to other zooming factors as well.

[2] Generally speaking, to obtain a lower resolution image, the higher resolution image is first low-pass-filtered and then subsampled. The low-pass filtering is necessary to prevent aliasing, see [12].

However, in practice, I_0 is unknown, and therefore L_0 is unknown too. If an approximation to L_0, $\tilde{L}_0$, can be found without the knowledge of I_0, then (1) can be approximated as

$$\hat{I}_0 = \tilde{I}_0 + \tilde{L}_0. \tag{2}$$

If $\tilde{L}_0$ is chosen properly, then $\hat{I}_0$ will be closer to I_0 than $\tilde{I}_0$ is, and therefore a more accurate magnification of the image can be achieved using a traditional technique in combination with an estimation of the difference image $\tilde{L}_0$ using (2). It is based on this rationale that a new technique for improving the performance of traditional image magnification methods is introduced. In the next section, we shall describe in detail this technique. The technique used to obtain $\tilde{L}_0$ is described in Section 4.

3. A NEW TECHNIQUE FOR IMAGE MAGNIFICATION BASED ON MULTIRESOLUTION REPRESENTATION

Based on the principles discussed in Section 2, we now describe a new technique for improving the performance of traditional image magnification methods. The schematic diagram of the method is shown in Fig. 3. To keep the notations consistent, the image to be magnified is denoted as I_1. The input image is first magnified by a factor of 2 in both directions using a traditional method to produce $\tilde{I}_0$, and at the same time, the input image is reduced by the same technique to produce I_2, which is again reduced to I_3. I_3 is then magnified and subtracted from I_2 to create L_2. I_2 is also magnified and subtracted from the input image to produce L_1. Then, L_1 and L_2 are used to generate a look-up table. By using table look-up, an estimation of the difference image, $\tilde{L}_0$, is obtained. Finally, the improved magnified image is obtained by summing $\tilde{I}_0$ and $\tilde{L}_0$ together.

The rationale of the scheme in Fig. 3 is the assumption that there is an underlining relationship between two adjacent levels of the image in the pyramid, and this relationship is roughly the same for all levels. Let X be a $2^{m-1} \times 2^{n-1}$ array and Y a $2^m \times 2^n$ array. Let

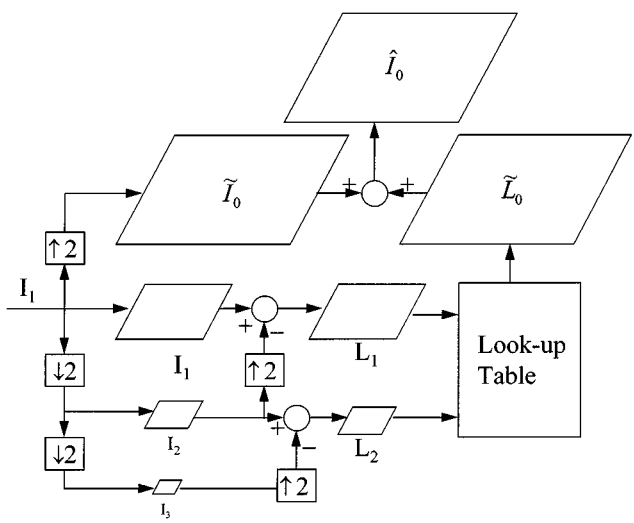

FIG. 3. A new technique for improving image magnification.

FIG. 4. Similar visual appearances of images at different resolutions.

$\Psi(X)$ be a function of X, which maps X to Y; i.e.,

$$Y = \Psi(X). \tag{3}$$

By choosing the function $\Psi(X)$ properly, $\Psi(X)$ may be used to estimate an approximation of a high-resolution image from a lower resolution image in Fig. 3,

$$L_1 = \Psi(L_2) + \varepsilon_1, \tag{4}$$

where ε_1 is the mapping error for level 1.

From Fig. 3, it can be seen that both L_1 and L_2 are known, and the mapping function $\Psi(X)$ can be estimated using these two images by solving

$$\Psi = \arg \min_{\forall \Psi} \|L_1 - \Psi(L_2)\|, \tag{5}$$

where $\|\cdots\|$ is the Euclidean norm.

Based on the assumption that there is an underlining relationship between two adjacent levels of the image in the pyramid which is roughly the same for all levels,[3] once $\Psi(X)$ has been found, it can be used to estimate $\tilde{L}_0$ as

$$\tilde{L}_0 = \Psi(L_1). \tag{6}[4]$$

[3] It is important to note that this assumption is informal; therefore we say the mapping relationship is roughly the same for different levels. This informal assumption can be justified by viewing the pyramid images at different levels. An example is shown in Fig. 4, where the visual appearances of these three levels of Laplacian images are seen to be very similar. This is also confirmed by extensive simulation results presented in Section 5. However, the exact mapping relationship will be resolution dependent, and may be impossible to find because of the lossy nature in the downsampling process.

[4] This equation does not imply the mapping relation from L_2 to L_1 and that of L_1 to L_0 are the same. It only means the mapping Ψ, found using L_2 and L_1 according to (5), can be used to *approximate* the mapping relationship from L_1 to L_0; i.e., it does not mean the mapping relationship is resolution independent.

In the next section we shall describe a method using vector quantization to implement the mapping.

4. INTERRESOLUTION IMAGE PREDICTION BASED ON VECTOR QUANTIZATION

4.1. The Interresolution Look-up Table (IRLUT)

From Section 3, it is clear that the mapping relation should be found using L_1 and L_2. A look-up table scheme is developed here to achieve this goal. We divide the images into small blocks for mapping. Let $X_{m+1}(i, j)$ be a $2^{k-1} \times 2^{l-1}$ block in L_{m+1}, $Y_m(i, j)$ be a $2^k \times 2^l$ block in L_m, and $\tilde{Y}_m(i, j)$ be an approximation to $Y_m(i, j)$, where i and j are the co-ordinates of the blocks. The look-up table mapping, which we shall call a interresolution look-up table, is illustrated in Fig. 5, where the encoder is a table of N entries whose single entry $C_2(n)$ is a $2^{k-1} \times 2^{l-1}$ array; the decoder is also a table of N entries whose single entry $C_1(n)$ is a $2^k \times 2^l$ array.

There are two tables in this scheme; to follow the tradition of vector quantization [13], we call them encoder and decoder respectively. In normal VQ, the encoder and decoder tables are identical. In our application, both tables have the same number of codewords and there is a one-to-one correspondence between the codewords in both tables; i.e., $C_2(n)$ in the encoder table and $C_1(n)$ in the decoder table are the nth corresponding pair of codewords. However, the codeword in one table is different from its counterpart in another table; i.e., $C_1(n) \neq C_2(n)$.

For a given $2^{k-1} \times 2^{l-1}$ block, $X_{m+1}(i, j)$ in L_{m+1}, there exists a corresponding $2^k \times 2^l$ block, $Y_m(i, j)$ in L_m. Each $X_{m+1}(i, j)$ is used to find an approximation to $Y_m(i, j)$, $\tilde{Y}_m(i, j)$ using table look-up. The operation of the table look-up process is as follows. The input $X_{m+1}(i, j)$ is first encoded into an index $n_{(i,j)}$ through minimum distance mapping; i.e., $n_{(i,j)}$ is found by

$$\left\| X_{m+1}(i, j) - C_2\left(n_{(i,j)}\right) \right\| \leq \| X_{m+1}(i, j) - C_2(l) \|, \quad \text{for all } l = 1, 2, \ldots, N. \tag{7}$$

Then $n_{(i,j)}$ serves as an index for the output reproduction; i.e., an approximation to $Y_m(i, j)$,

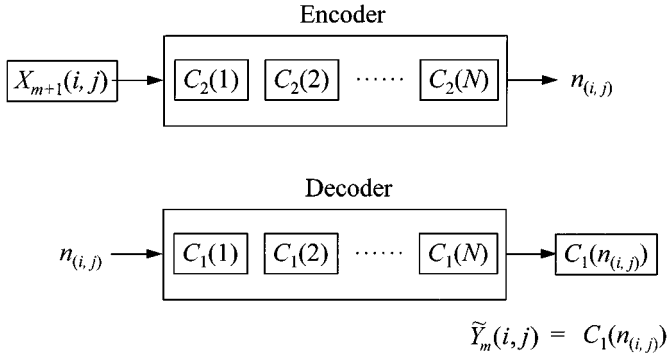

FIG. 5. Interresolution look-up table.

$\tilde{Y}_m(i, j)$ is found as

$$\tilde{Y}_m(i, j) = C_1\big(n_{(i,j)}\big). \tag{8}$$

Once the codewords in both tables in Fig. 5 are specified, the operation of the mapping process is completely described by (7) and (8). The remaining task, therefore, is to design the two tables.

4.2. IRLUT Design Algorithm

To create IRLUT, the encoder codebook is first designed using samples from L_2. There are many methods available for designing the codebook. One well-known method is the generalized Lloyd algorithm (GLA), which is also known as the Linde–Buzo–Gray (LBG) algorithm [13]. Recently, methods based on neural networks have become popular [14]. These algorithms have been well described elsewhere [13, 14]; readers not familiar with VQ can consult the references. Once the encoder codebook, $C_2(1), C_2(2), \ldots, C_2(N)$, is specified, the decoder codebook is decided as

$$C_1(l) = \frac{1}{|S_l|} \sum_{X_2(i,j)\in S_l} Y_1(i, j), \quad \text{for all } l = 1, 2, \ldots, N, \tag{9}$$

where $X_2(i, j)$ is a $2^{k-1} \times 2^{l-1}$ block in L_2, $Y_1(i, j)$ is the corresponding $2^k \times 2^l$ block in L_1, S_l is a subset of $2^{k-1} \times 2^{l-1}$ array, $|S_l|$ is the number of $X_2(i, j)$ in the subset S_l, and $X_2(i, j) \in S_l$ if

$$\|X_2(i, j) - C_2(l)\| \le \|X_2(i, j) - C_2(k)\|, \quad \text{for all } k. \tag{10}$$

5. EXPERIMENTAL RESULTS

To evaluate the performance of the proposed technique, computer simulations have been performed on many gray-level images. To provide some quantitative measures of the performance of different image magnification methods, the image is first downsized and then magnified back to its original size using different methods. In this way, the performance of different techniques can be evaluated by calculating the difference between the original signal and the magnified images. Letting $I_{\text{org}}(i, j)$ be the original image, and $I_{\text{mag}}(i, j)$ the magnified image, mean square error (MSE) and signal-to-noise ratio (SNR) calculated as follows are used to measure the performance of the magnification techniques

$$\text{MSE} = \frac{1}{M \times N} \sum_{i=1}^{M} \sum_{j=1}^{N} (I_{\text{org}}(i, j) - I_{\text{mag}}(i, j)) \tag{11}$$

$$\text{SNR} = 10 \log\left(\frac{\frac{1}{M\times N} \sum_{i=1}^{M} \sum_{j=1}^{N} I_{\text{org}}^2(i, j)}{\text{MSE}} \right) \text{dB}, \tag{12}$$

where M and N are the dimensions of the original image.

In the experiment, four different traditional methods for image reduction and expansion are implemented, and the new method is used to improve the results of these traditional techniques. The methods used are:

(1) Burt and Adelson's Gaussian filter [1] with $a = 0.4$, the filter coefficients are $\{0.05, 0.25, 0.4, 0.25, 0.05\}$.

(2) A wavelet filter pair [15]. The analysis low-pass filter used was a 9-tap filter: $\{0.037828, -0.023849, -0.110624, 0377402, 0.852699, 0.377402, -0.110624, -0.023849, 0.037828\}$, and the low-pass synthesis filter used was a 7-tap filter: $\{-0.064539, -0.040689, 0.418092, 0.788468, 0.418092, -0.040689, -0.064539\}$.

(3) Bilinear interpolation [5].

(4) Bicubic interpolation [12].

The image is first reduced by a factor of 2 and 4 in both dimensions by these 4 different methods respectively. The reduced image is then magnified back to its original resolution by the same method used to reduce the image. For implementation convenience, reduction/expansion factors of 4 are realized by reducing/expanding the image by a factor of 2 twice in succession.

In implementing the new method, lower resolution images are divided into 2×2 blocks, and each is mapped to a 4×4 block in its next higher resolution image. The choice of these block sizes is for implementation convenience; other block sizes are possible.

Because the mapping is a few-to-many mapping, it is important to use enough data to design the look-up table. Also, due to the added complexity of the new method, the look-up table should be estimated offline. These two considerations can be resolved by using many sample images to train the look-up table. In the results presented here four gray scale images, Baboon, Boat, Lena, and Peppers as shown in Fig. 6 are used to design the

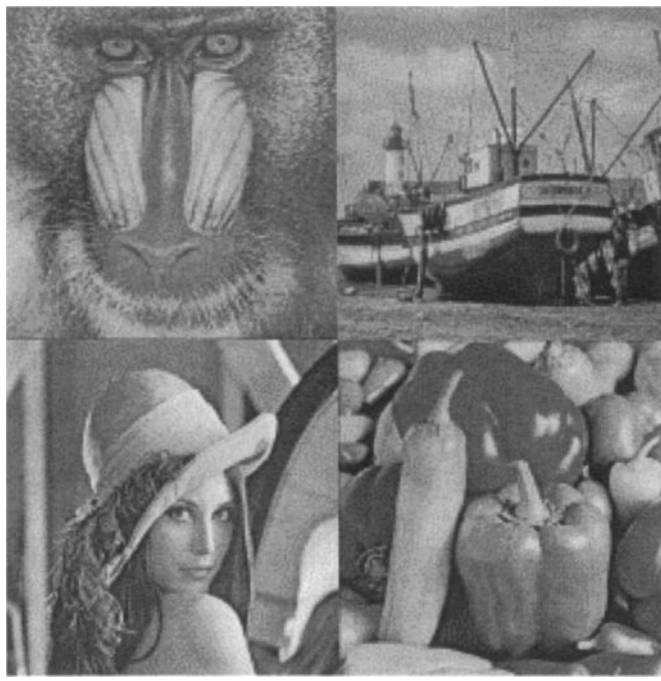

FIG. 6. Images used to train the look-up tables.

TABLE I
Comparison of the MSE and SNR Performances of Gaussian Pyramid Image Expansion Method and the New Improved Method

	Reduce/expansion factors			
	2 (512×512 to 256×256 and 256×256 to 512×512)		4 (512×512 to 128×128 and 128×128 to 512×512	
Images	Original method	Improved	Original method	Improved
Detergent	200.9 (17.7 dB)	156.9 (18.7 dB)	424.9 (14.4 dB)	364.5 (15.1 dB)
MRI	363.8 (14.8 dB)	256.9 (16.4 dB)	908.3 (10.9 dB)	742.1 (11.7 dB)
Lena	79.5 (23.5 dB)	52.8 (25.3 dB)	238.8 (18.7 dB)	160.5 (20.4 dB)
Baboon	325.9 (17.3 dB)	286.9 (17.9 dB)	491.6 (15.5 dB)	462.5 (15.8 dB)

Note. The numbers inside the brackets are SNR values.

look-up table. The original sizes of these images are 512×512 pixels. The mapping tables are designed using the 128×128 and 256×256 difference images. One table is designed for each of the four traditional methods. The number of entries in the tables is chosen to be 512. Obviously, a larger table may provide better mapping accuracy, but will be computationally more demanding; a smaller table will be computationally faster but may be less accurate.

Numerical results on four images, two inside the training set (Lena and Baboon) and two outside the training set (MRI and Detergent) are shown in Tables I to IV. It should be noted that for each method, only one interresolution look-up table, designed using data of 128×128 and 256×256 difference images of Fig. 6, is used to expand all images from

TABLE II
Comparison of the MSE and SNR Performances of Wavelet Image Expansion Method and the New Improved Method

	Reduce/expansion factors			
	2 (512×512 to 256×256 and 256×256 to 512×512)		4 (512×512 to 128×128 and 128×128 to 512×512	
Images	Original method	Improved	Original method	Improved
Detergent	137.6 (19.3 dB)	124.1 (19.8 dB)	383.0 (14.9 dB)	338.1 (15.4 dB)
MRI	242.6 (16.6 dB)	186.5 (17.7 dB)	826.7 (11.3 dB)	674.3 (12.3 dB)
Lena	56.2 (25.0 dB)	37.9 (26.7 dB)	215.0 (19.2 dB)	133.5 (21.2 dB)
Baboon	262.8 (18.2 dB)	254.7 (18.4 dB)	496.4 (15.7 dB)	444.1 (15.9 dB)

Note. The numbers inside the brackets are SNR values.

TABLE III
Comparison of the MSE and SNR Performances of Bicubic Image Expansion Method and the New Improved Method

	Reduce/expansion factors			
	2 (512 × 512 to 256 × 256 and 256 × 256 to 512 × 512)		4 (512 × 512 to 128 × 128 and 128 × 128 to 512 × 512	
Images	Original method	Improved	Original method	Improved
Detergent	162.1 (18.6 dB)	109.0 (20.3 dB)	373.7 (14.9 dB)	293.3 (16.0 dB)
MRI	250.2 (16.5 dB)	163.1 (18.3 dB)	710.9 (11.9 dB)	538.4 (13.1 dB)
Lena	60.7 (24.6 dB)	40.2 (26.4 dB)	184.9 (19.8 dB)	139.9 (21.0 dB)
Baboon	455.4 (15.8 dB)	306.5 (17.6 dB)	446.7 (15.9 dB)	402.4 (16.4 dB)

Note. The numbers inside the brackets are SNR values.

256 × 256 to 512 × 512 and 128 × 128 to 512 × 512. From these results, it is seen the new method has improved all the traditional methods for all the images and different factors of expansion.

The new method not only improves the numerical results, it also improves the visual sharpness of the expanded images. Some examples of the results are shown in Figs. 7 to 11. Since the bilinear method provides consistently the best MSE performance for all the images and factors, only images generated by this method and its improved versions are shown. From these results, it is seen the new technique improves the sharpness of the magnified images.

TABLE IV
Comparison of the MSE and SNR Performances of Bilinear Image Expansion Method and the New Improved Method

	Reduce/expansion factors			
	2 (512 × 512 to 256 × 256 and 256 × 256 to 512 × 512)		4 (512 × 512 to 128 × 128 and 128 × 128 to 512 × 512	
Images	Original method	Improved	Original method	Improved
Detergent	115.1 (20.1 dB)	95.1 (20.9 dB)	308.9 (15.8 dB)	270.3 (16.4 dB)
MRI	167.5 (18.2 dB)	135.2 (19.1 dB)	565.6 (12.9 dB)	480.4 (13.6 dB)
Lena	39.8 (26.5 dB)	32.4 (27.4 dB)	144.1 (20.9 dB)	115.3 (21.9 dB)
Baboon	232.2 (18.8 dB)	205.5 (19.3 dB)	417.4 (16.2 dB)	383.1 (16.6 dB)

Note. The numbers inside the brackets are SNR values.

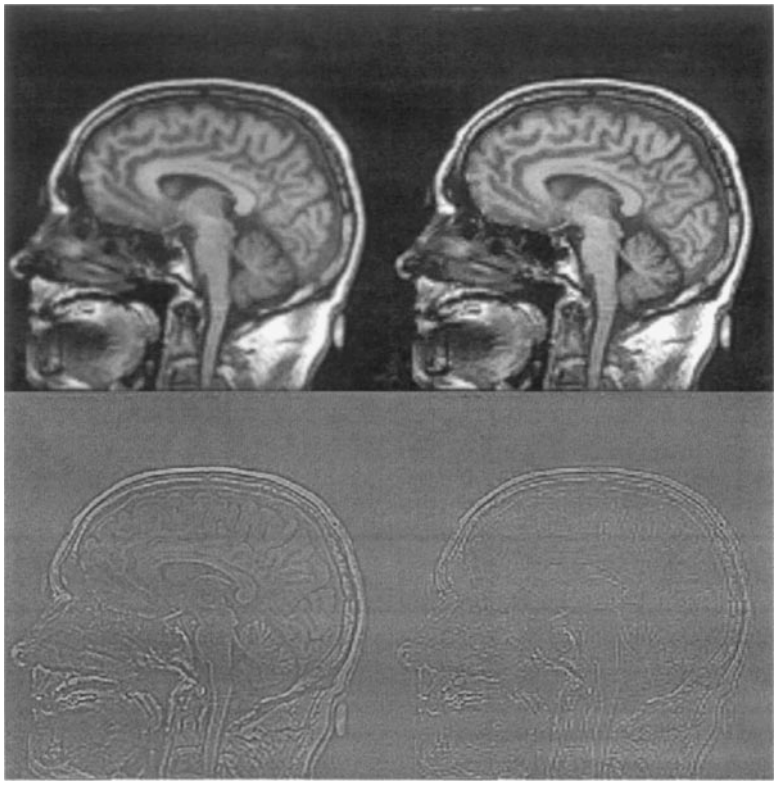

FIG. 7. MRI image reduced and then expanded by a factor of 2 (256×256 to 128×128 and 128×128 to 256×256). Top left: bilinear interpolation. Top right: Image improved by the new method. Bottom left: Difference image of bilinear interpolation. Bottom right: Difference image of improved method.

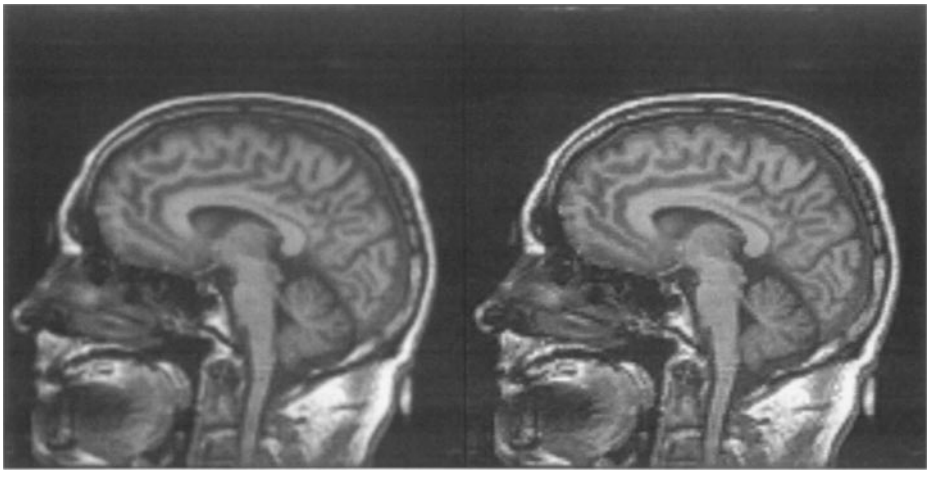

FIG. 8. MRI image reduced and then expanded by a factor of 4 (512×512 to 128×128 and 128×128 to 512×512). Left: Bilinear interpolation. Right: Image improved by new method.

FIG. 9. Detergent image reduced and then expanded by a factor of 4 (512×512 to 128×128 and 128×128 to 512×512). Left: Bilinear interpolation. Right: Image improved by new method.

FIG. 10. Lena image reduced and then expanded by a factor of 4 (512×512 to 128×128 and 128×128 to 512×512). Left: Bilinear interpolation. Right: Image improved by new method.

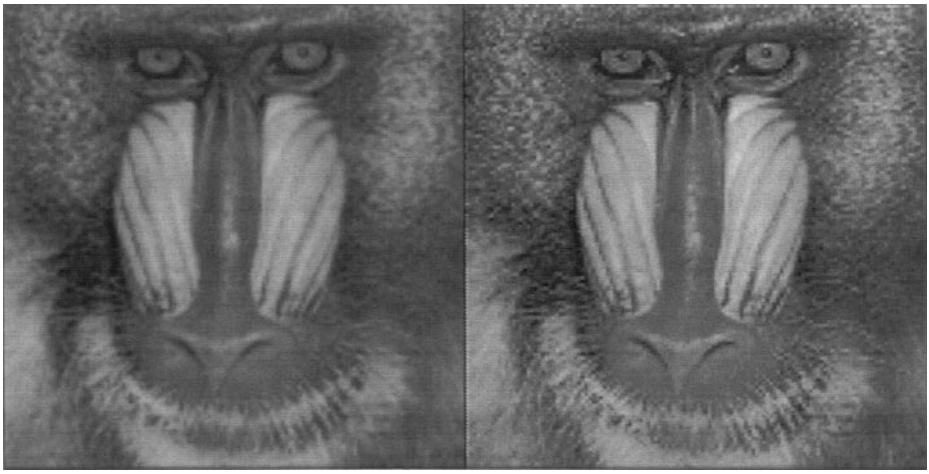

FIG. 11. Baboon image reduced and then expanded by a factor of 4 (512×512 to 128×128 and 128×128 to 512×512). Left: Bilinear interpolation. Right: Image improved by new method.

The new method can be used in combination with any previously known image magnification method and similar improvements have been consistently observed.

6. CONCLUSIONS

In this paper, an improved image magnification scheme has been described. Simulation results have been presented which show the new method improves the performance of traditional magnification methods in terms of both better visual quality of the magnified image and lower reconstruction error. The nice characteristic of the current method is that it can be used in combination with any existing image magnification method to improve its performance. Since many image processing packages implement at least one zooming method, the technique developed in this work can be easily incorporated into existing software packages. The important contribution of this work is the technique for improving spatial magnification of images. Only one possible mapping method is studied in this paper. Better mapping strategies may exist, and we are currently investigating in this direction.

ACKNOWLEDGMENT

The author expresses his sincere gratitude to the three anonymous reviewers for their valuable comments and suggestions.

REFERENCES

1. P. J. Burt and E. H. Adelson, The Laplacian pyramid as a compact image code, *IEEE Trans. Commun.* **31**, 1983, 532–540.
2. C. L. Huang and K. C. Chen, Directional moving averaging interpolation for texture mapping, *Graphics Models Image Process.* **58**, 1996, 301–313.
3. Y. Y. Tang and C. Y. Suen, Image transformation approach to nonlinear shape restoration, *IEEE Trans. Syst. Man Cybernet.* **23**, 1993, 155–172.
4. D. M. Martinez and J. S. Lim, Spatial interpolation of interlaced television pictures, in *Proceedings of ICASSP'89, May 1989*, pp. 1886–1889.
5. A. K. Jain, *Fundamentals of Digital Image Processing*, Prentice Hall, Englewood Cliffs, NJ, 1989.
6. J. A. Parker, R. V. Kenyon, and D. E. Troxel, Comparison of interpolating methods for image resampling *IEEE Trans. Medical Imaging* **2**, 1983, 31–39.
7. H. S. Hou and H. C. Andrews, Cubic spline for image interpolation and digital filtering, IEEE Trans. *Acoust. Speech Signal Process.* **26**, 1978, 508–517.
8. M. Unser, A. Aldroubi, and M. Eden, Enlargement and reduction of digital images with minimum loss of information, *IEEE Trans. Image Process.* **4**, 1995, 247–258.
9. R. R. Schultz and R. L. Stevenson, A Bayesian approach to image expansion for improved definition, *IEEE Trans. Image Process.* **3**, 1994, 233–242.
10. K. Jensen and D. Anastassiou, Sub-pixel edge localization and interpolation of still image, *IEEE Trans. Image Process.* **4**, 1995, 285–295.
11. R. C. Gonzalez and R. E. Woods, *Digital Image Processing*, Addison-Wesley, Reading, MA, 1993.
12. W. P. Pratt, *Digital Image Processing*, Wiley, New York, 1992.
13. A. Gersho and R. M. Gray, *Vector Quantization and Signal Compression*, Kluwer, Dordrecht, 1991.
14. J. Hertz, A. Krogh, and R. G. Palmer, *Introduction to the Theory of Neural Computation*, Addison-Wesley, Reading, MA, 1991.
15. J. D. Villasenor, B. Belzer, and J. Liao, Wavelet filter evaluation for image compression, *IEEE Trans. Image Process.* **4**, 1995, 1053–1060.

GUOPING QIU received the B.Sc. in electronic measurement and instrumentation from the University of Electronic Science and Technology of China, in 1984, and the Ph.D. in electrical and electronic engineering from the University of Central Lancashire, Preston, England, in 1993. In 1993, he joined the School of Computing and Mathematics at the University of Derby, England, as a lecturer, and moved to the School of Computer Studies at the University of Leeds, England, 1999, where he is also a lecturer. His research interest is the general aspects of visual information processing, including color imaging, image coding, enhancement, image database, image processing, and computer vision for industrial inspection and WWW-based informatics.